J Physiol Sci (2016) 66:387–396
DOI 10.1007/s12576-016-0435-6

ORIGINAL PAPER

Inhibition of monocarboxylate transporter 1 suppresses the proliferation of glioblastoma stem cells

Tetsuya Takada[1] · Kazuyuki Takata[1] · Eishi Ashihara[1]

Received: 6 January 2016 / Accepted: 26 January 2016 / Published online: 22 February 2016

Abstract Recent evidence suggests that a minor subset of cancer cells, termed cancer stem cells (CSCs), have self-renewal and tumorigenic potential. Therefore, the characterization of CSCs is important for developing therapeutic strategies against cancer. Cancer cells rely on anaerobic glycolysis to produce ATP even under normoxic conditions, resulting in the generation of excess acidic substances. Cancer cells maintain a weakly alkaline intracellular pH to support functions. Glioblastoma is an aggressive malignancy with a poor 5-year survival rate. Based on the hypothesis that ion transport-related molecules regulate the viability and function of CSCs, we investigated the expression of ion transport-related molecules in glioblastoma CSCs (GSCs). Quantitative RT-PCR analysis showed that monocarboxylate transporter1 (MCT1) were upregulated in GSCs, and inhibition of MCT1 decreased the viability of GSCs compared with that of non-GSCs. Our findings indicate that MCT1 is involved in the maintenance of GSCs and is a promising therapeutic target for glioblastoma.

Keywords Glioblastoma · Cancer stem cell · Hypoxia · Monocarboxylate transporter · Lactic acid · Carbonic anhydrase

Abbreviations

ATP	Adenosine triphosphate
b-FGF	Basic fibroblast growth factor
CA	Carbonic anhydrase
CSC	Cancer stem cell
DMEM	Dulbecco's modified Eagle's medium
DMSO	Dimethyl sulfoxide
EGF	Epidermal growth factor
FBS	Fetal bovine serum
GSC	Glioblastoma cancer stem cell
HA	Hypoxia-adapted
MCT	Monocarboxylate transporter
NHE	Na^+–H^+ exchanger
PC/SM	Penicillin/streptomycin
pHMBS	*p*-hydroxymercuribenzoic acid sodium salt
qRT-PCR	Quantitative reverse transcription polymerase chain reaction
RT	Room temperature
UPL	Universal probe library

Introduction

A subpopulation of tumor cells with the properties of stem cells, including self-replication ability and pluripotency, have been identified and termed cancer stem cells (CSCs). The CSC hypothesis states that tumors show a hierarchical organization based on the supply of cells from CSCs. Furthermore, CSCs are resistant to current anticancer drugs and radiation and play an important role in metastasis [1–4].

Glioma is the most common primary brain tumor. Glioblastoma is an aggressive form of this tumor and has a

Electronic supplementary material The online version of this article (doi:10.1007/s12576-016-0435-6) contains supplementary material, which is available to authorized users.

✉ Eishi Ashihara
ash@mb.kyoto-phu.ac.jp

[1] Department of Clinical and Translational Physiology, Kyoto Pharmaceutical University, 5 Nakauchi, Yamashina-ku, Kyoto 607-8414, Japan

poor prognosis, with a 5-year survival rate of ≤5 % [5]. A cell population known as glioblastoma stem cells (GSCs) is involved in the maintenance of glioblastomas [6, 7] as well as resistance to chemotherapies [8, 9]. Therefore, we have to develop novel molecular strategies against GSCs.

Cancer cells rely on anaerobic glycolysis for energy production even in the presence of oxygen in what is termed the Warburg effect [10, 11]. Glioblastoma cells produce ATP via the Warburg effect [12], resulting in the production of acidic substances, such as carbon dioxide and lactic acid, which accumulate as metabolites in the cytoplasm. Protons and metabolites associated with acidic substances are released by cancer cells to the extracellular space or accumulate in acidic granules, and cell function is preserved through the maintenance of a weakly alkaline intracellular environment. The acidity of the cancer microenvironment is thought to contribute to malignant progression and drug resistance [13]. Ion transport-related molecules, such as carbonic anhydrase (CA), Na^+–H^+ exchanger (NHE), and monocarboxylate transporter (MCT), are responsible for this function and are expressed at higher levels in cancer cells than in normal cells [14–20].

Here, we hypothesized that enhanced anaerobic glycolysis in CSCs, which are abundant in the hypoxic environment, results in the production of excess acidic substances [21]. We therefore examined the expression and activity of ion transport-related molecules that release protons to the extracellular medium.

Materials and methods

Cell culture

The glioblastoma cell lines U-251 MG (mutant p53) and U-87 MG (wild-type p53) were purchased from the American Type Culture Collection and cultured in Dulbecco's modified Eagle's medium (DMEM)/low glucose (Wako, Osaka, Japan) containing 10 % fetal bovine serum (FBS; Sigma-Aldrich, St. Louis, MO, USA) and 1 % penicillin/streptomycin (PC/SM; Wako) (DMEM/low) in a CO_2 incubator [MCO-18AIC (UV); SANYO Electric, Osaka, Japan] with 5 % CO_2 at 37 °C for normoxia or in a O_2/CO_2 incubator (WKN-9200EX; Waken Btech, Kyoto, Japan) with 1 % O_2 and 5 % CO_2 at 37 °C for hypoxia. Hypoxia-adapted (HA) cells were those incubated for at least 1 month under hypoxic conditions. Cells were seeded at a density of 5.0×10^4 cells/ml. We defined that non-CSCs normoxia were adherent cells incubated under normoxic conditions, and non-CSCs hypoxia were adherent cells incubated under hypoxic conditions.

CSC preparation

CSCs were prepared by the sphere formation assay, in which cells were cultured in DMEM/F12 (Thermo Fisher Scientific, Waltham, MA, USA) containing 1 % PC/SM, 2 % B-27 [B-27® Serum-Free Supplement (50×); Thermo Fisher Scientific], 20 ng/ml epidermal growth factor (EGF; Peprotech, Rocky Hill, NJ, USA), and 20 ng/ml basic fibroblast growth factor (b-FGF; Peprotech) for 7 days in ultra-low attachment 6-well plates (Corning International, Corning, NY, USA). EGF and b-FGF were added at 20 ng/ml on day 3. U-251 MG cells were seeded at a density of 1.0×10^5 cells/ml. U-87 MG cells were seeded at a density of 6.7×10^4 cells/ml. We defined that CSCs normoxia were spheres incubated under normoxic conditions.

Immunofluorescence analysis

Adherent cells (non-CSCs) were cultured in DMEM/low in glass-bottom microwell dishes (P35G-1.5-14-C; MatTek, Ashland, MA, USA) for 3 days. After culture, cells were fixed in 4 % paraformaldehyde (PFA; Nacalai Tesque, Kyoto, Japan) for 30 min, and then incubated with primary antibodies (rabbit polyclonal anti-human Nanog, 1:500; Merck Millipore, Billerica, MA, USA; rabbit monoclonal anti-human Nestin, 1:100; Abcam, Cambridge, UK; and mouse monoclonal anti-human CD133/1, W6B3C1, 1:50; Miltenyi Biotec, Bergisch Gladbach, Germany) overnight at room temperature (RT). Cells were then incubated with secondary antibody (1:500) (Alexa Fluor 488 anti-rabbit IgG or Alexa Fluor 488 anti-mouse IgG; Thermo Fisher Scientific) for 2 h at 4 °C. Nuclei were stained with Hoechst33342 (1:10,000) (Thermo Fisher Scientific).

To produce sphere (CSCs) samples, cells were harvested and fixed in 50 % methanol for 10 min at RT with shaking (60 rpm), and 2 % PFA for 20 min at RT with shaking (60 rpm). After fixing, cells were incubated with primary antibody (same concentrations) overnight at RT with shaking (60 rpm), followed by incubation with secondary antibody (1:500) for 2 h at 4 °C with shaking (60 rpm). Cells were then suspended in mount medium (VECTASHIELD; Vector Laboratories, Burlingame, CA, USA) and seeded on microscope slides with a cover glass (CoverWell™ Imaging Chambers PCI-A-0.5; Grace Bio-Labs, Bend, OR, USA).

For staining of hypoxic areas, cells were treated with pimonidazole HCl (200 μM) for 2 h before harvesting and then stained with anti-pimonidazole mouse IgG_1 monoclonal antibody (clone 4.3.11.3) (1:50) (Hypoxyprobe™-1 Kit; Hypoxyprobe, Burlington, MA, USA). Samples were visualized using a confocal laser scanning microscope (LSM 510 META; Carl Zeiss, Oberkochen, Germany). ImageJ software was used for image analysis.

Quantitative reverse transcription polymerase chain reaction (qRT-PCR)

Total RNA was extracted with the Illustra RNAspin Mini RNA Isolation Kit (GE Healthcare UK, Little Chalfont, Bucks, UK) following the manufacturer's protocol. RNA was quantified using NanoDrop 2000 (Thermo Fisher Scientific). Then, cDNA was synthesized using the High-Capacity cDNA Reverse Transcription Kit (Thermo Fisher Scientific) following the manufacturer's protocol. The concentration was adjusted to 20 ng/μl.

qRT-PCR was performed on a 7500 Real-Time PCR System (Thermo Fisher Scientific) with a FastStart Universal Probe Master (Rox) (Roche Applied Science, Penzberg, Germany). The relative expression of the selected genes was normalized to that of 18S rRNA for each sample. As a control, 5 ng of cDNA (total RNA substantial amount) was used per response. Templates were amplified under the following conditions: 95 °C for 10 min, and then 40 cycles of 95 °C for 15 s and 60 °C for 1 min. The combinations of various primer sets (Thermo Fisher Scientific) and probes (Roche Applied Science) are shown in Supplementary Table S1. The primer sequences and probes were determined using Universal Probe Library (UPL) (https://qpcr.probefinder.com/organism.jsp).

Inhibitor preparation

p-hydroxymercuribenzoic acid sodium salt (pHMBS; Sigma-Aldrich) was dissolved in sterile milliQ to a concentration 15 mM, and diluted with medium to achieve working concentrations. AR-C117977 was dissolved in dimethyl sulfoxide (DMSO; Wako) to a stock concentration of 100 mM, and diluted with medium to reach working concentrations. DMSO was used at a concentration of 0.2 %.

WST-8 assay

The cytostatic effect of MCT inhibitors (pHMBS, AR-C117977) on adherent cells was determined using the WST-8 assay. Cells were seeded at a density of 3.0×10^3 cells/90 μl per well in 96-well cell culture plates (Corning International) and treated with inhibitors (10 μl per well) at 24 h after seeding. After 72 h, the Cell Count Reagent SF (Nacalai Tesque) was added at 10 μl per well, and plate were placed in a CO_2 incubator for 3 h. Absorbance was measured at 450 nm (reference wavelength: 630 nm) with a microplate reader (Model 680 Microplate Reader; Bio-Rad, Hercules, CA, USA).

CellTiter-Glo® 3D cell viability assay

The cytostatic effect of MCT1 inhibitors on spheres was determined using the CellTiter-Glo® 3D cell viability assay. Cells were seeded at a density of 3.0×10^3 cells/90 μl per well in ultra-low attachment 96-well plates (Corning International) and treated with inhibitors (10 μl per well) at 24 h after seeding. After 6 days, the cell-containing media were transferred to a 96-well white plate (96F Nunclon™ Delta White Microwell SI; Thermo Fisher Scientific). CellTiter-Glo® 3D Reagent (Promega, Madison, WI, USA) was added at 100 μl per well, mixed by shaking for 5 min, and incubated for 25 min at RT. Luminescence was measured with a luminometer (GloMax® Discover System; Promega).

Lactate assay

The cells were harvested and suspended in PBS, and solutions were disrupted to generate intracellular lactate samples using Handy Sonic (UR-20P; Tomy Seiko, Tokyo, Japan). A Lactate Assay Kit II (BioVision, Milpitas, CA, USA) was used for measurements following the manufacturer's protocol. Absorbance was measured at 450 nm with a microplate reader (GloMax® Discover System).

Statistical analysis

The differences in stem cell marker mRNA expression levels or inhibitor effects between non-CSCs and CSCs were analyzed using the Student's *t* test. The differences in ion transport-related molecule mRNA expression levels between non-CSCs normoxia, non-CSCs hypoxia, and CSCs normoxia were analyzed using the Tukey–Kramer test. The Smirnov-Grubbs' test was used to evaluate the outliers of ion transport-related molecule mRNA expression levels. Statistical analyses were performed using Statview software for Windows (SAS Institute, Cary, NC, USA).

Results

Obtainment of CSCs using the sphere formation assay

CSCs of U-251 MG and U-87 MG cells were generated using the sphere formation assay, and the formation of spheres was confirmed by an inverted microscope (IX70 Olympus, Tokyo, Japan) (Fig. 1a). The sphere-forming assay is a common technique used to examine the function of cancer stem cells [22, 23]. Tumor cells almost die in the

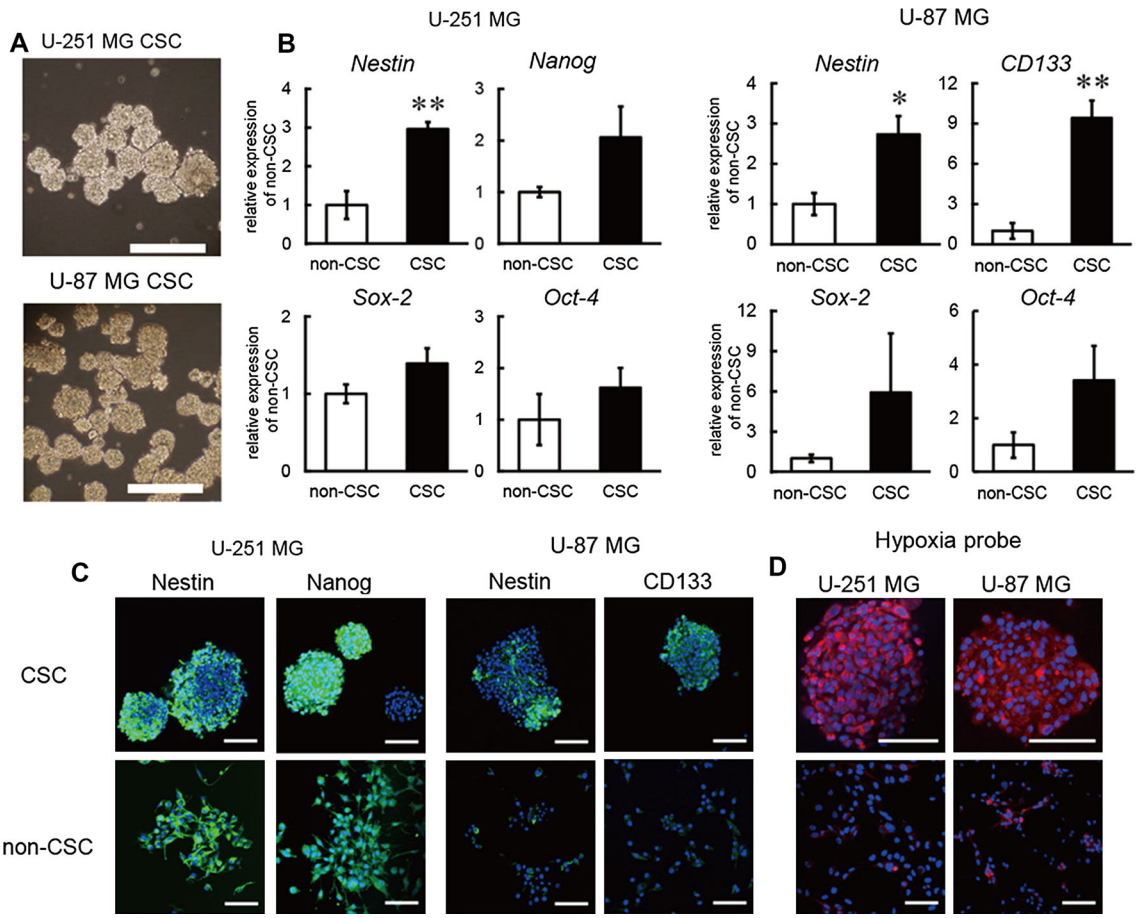

Fig. 1 Generation of CSCs by the sphere formation assay. **a** Glioblastoma cell lines (U-251 MG and U87-MG) formed spheres by the sphere formation assay (*scale bars* 200 μm). **b** Stem cell marker (*Nestin*, *Nanog*, *CD133*, *Sox-2*, and *Oct-4*) mRNA expression levels were increased in CSCs. *18S rRNA* was used as an internal control ($n = 3$, mean ± SEM; $^{*}p < 0.05$, $^{**}p < 0.01$ vs. non-CSC). **c**, **d** Immunofluorescence analysis shows that the expression of stem cell markers was increased in spheres. Pimonidazole, a hypoxia probe, accumulated in spheres (*scale bars* 100 μm). *CSC* cancer stem cell

process of forming spheres (when cultured under non-adherent conditions), and cancer stem cells proliferate. Total RNA was extracted from spheres, and the mRNA levels of stem cell markers (*Nestin*, *Nanog*, *CD133*, *Sox-2*, and *Oct-4*) were compared between adherent cells and spheres cultured in 20 % O_2 by qRT-PCR. *Nestin* was upregulated in U-251 MG cells, and *Nestin* and *CD133* were upregulated in U-87 MG cells (Fig. 1b). Immunofluorescence analysis using a confocal laser microscope showed the upregulation of Nestin and Nanog in U-251 MG cells, and the upregulation of Nestin and CD133 in U-87 MG cells (Fig. 1c). Therefore, a population of cells containing many stem cells was obtained using the sphere formation assay. In the following experiments, spheres were considered CSCs and adherent cells were considered non-CSCs.

In addition, spheres were treated with pimonidazole, which is reduced under hypoxic conditions and aggregates in cells. The accumulation of pimonidazole in spheres was confirmed by immunofluorescence staining, indicating that intracellular conditions were hypoxic (Fig. 1d).

The mRNA expression levels of ion transport-related molecules in non-CSCs and CSCs

To analyze the changes in the mRNA expression levels of ion transport-related molecules, samples of non-CSCs normoxia, CSCs normoxia, and non-CSCs hypoxia were prepared and subjected to qRT-PCR. The following transport-related molecules were analyzed: CA (CA9, CA12), NHE (NHE1, NHE2), and MCT (MCT1, MCT4). *CA9* and *CA12* mRNA transcripts were upregulated in HA cells and CSCs in both cell lines (U-251 MG; *CA9* in HA cells: 26.12 ± 2.34, *CA9* in CSCs: 38.91 ± 5.84, *CA12* in HA cells: 3.30 ± 1.20, *CA12* in CSCs: 44.58 ± 4.95, U-87 MG; *CA9* in HA cells: 21.47 ± 2.27, *CA9* in CSCs: 23.42 ± 5.20, *CA12* in HA cells: 1.61 ± 0.18, *CA12* in CSCs: 3.61 ± 0.70). In the U-251 MG cells, both *NHE1* and NHE2 transcripts were downregulated in HA cells and CSCs, whereas *NHE2* was upregulated in CSCs in U-87 MG cells (U-251 MG; *NHE1* in HA cells: 0.66 ± 0.10, *NHE1* in CSCs: 0.22 ± 0.01, *NHE2* in HA cells:

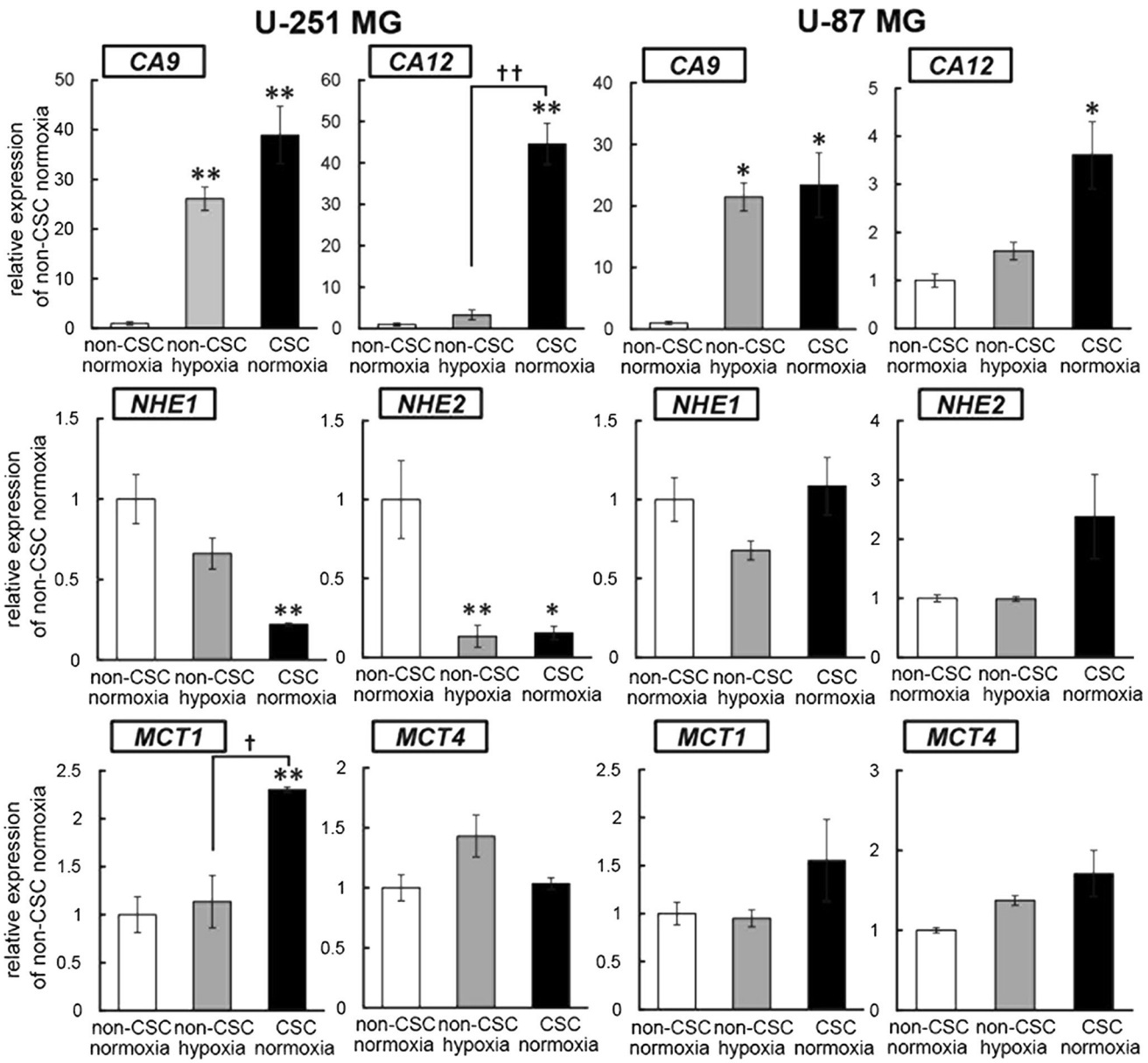

Fig. 2 mRNA expression of ion transport-related molecules in non-CSCs normoxia (*white bars*), non-CSCs hypoxia (*gray bars*), and CSCs normoxia (*black bars*). *CA9* and *CA12* transcripts were upregulated by hypoxia in U251-MG and U87-MG cell lines. *CA9*, *CA12*, and *MCT1* transcripts were upregulated by CSCs in these cell lines ($n = 3$–5, mean ± SEM; $^{*}p < 0.05$, $^{**}p < 0.01$ vs. non-CSC normoxia. $^{\dagger}p < 0.05$, $^{\dagger\dagger}p < 0.01$ vs. non-CSC hypoxia). *CSC* cancer stem cell, *CA* carbonic anhydrase, *NHE* Na^{+}–H^{+} exchanger, *MCT* monocarboxylate transporter

0.13 ± 0.07, *NHE2* in CSCs: 0.15 ± 0.04, U-87 MG; *NHE1* in HA cells: 0.67 ± 0.06, *NHE1* in CSCs: 1.09 ± 0.18, *NHE2* in HA cells: 0.99 ± 0.04, *NHE2* in CSCs: 2.38 ± 0.71). *MCT1* and *MCT4* was upregulated slightly in CSCs in U-87 MG cells, and *MCT1* was upregulated in CSCs in U-251 MG cells (U-251 MG; *MCT1* in HA cells: 1.14 ± 0.27, *MCT1* in CSCs: 2.30 ± 0.03, *MCT4* in HA cells: 1.43 ± 0.17, *MCT4* in CSCs: 1.04 ± 0.05, U-87 MG; *MCT1* in HA cells: 0.95 ± 0.09, *MCT1* in CSCs: 1.55 ± 0.43, *MCT4* in HA cells: 1.37 ± 0.06, *MCT4* in CSCs: 1.71 ± 0.29) (Fig. 2). Based on these observations, we were focused on MCT1, which were upregulated in CSCs to a greater extent than in HA cells.

The pHMBS (MCT inhibitor) was more cytotoxic at lower concentrations in CSCs than in non-CSCs in U-251 MG cells and inhibited sphere formation

To analyze the effects of MCT inhibition, non-CSCs or CSCs of U-251 MG and U-87 MG cells were treated with pHMBS. The IC_{50} was approximately 260 μM in non-

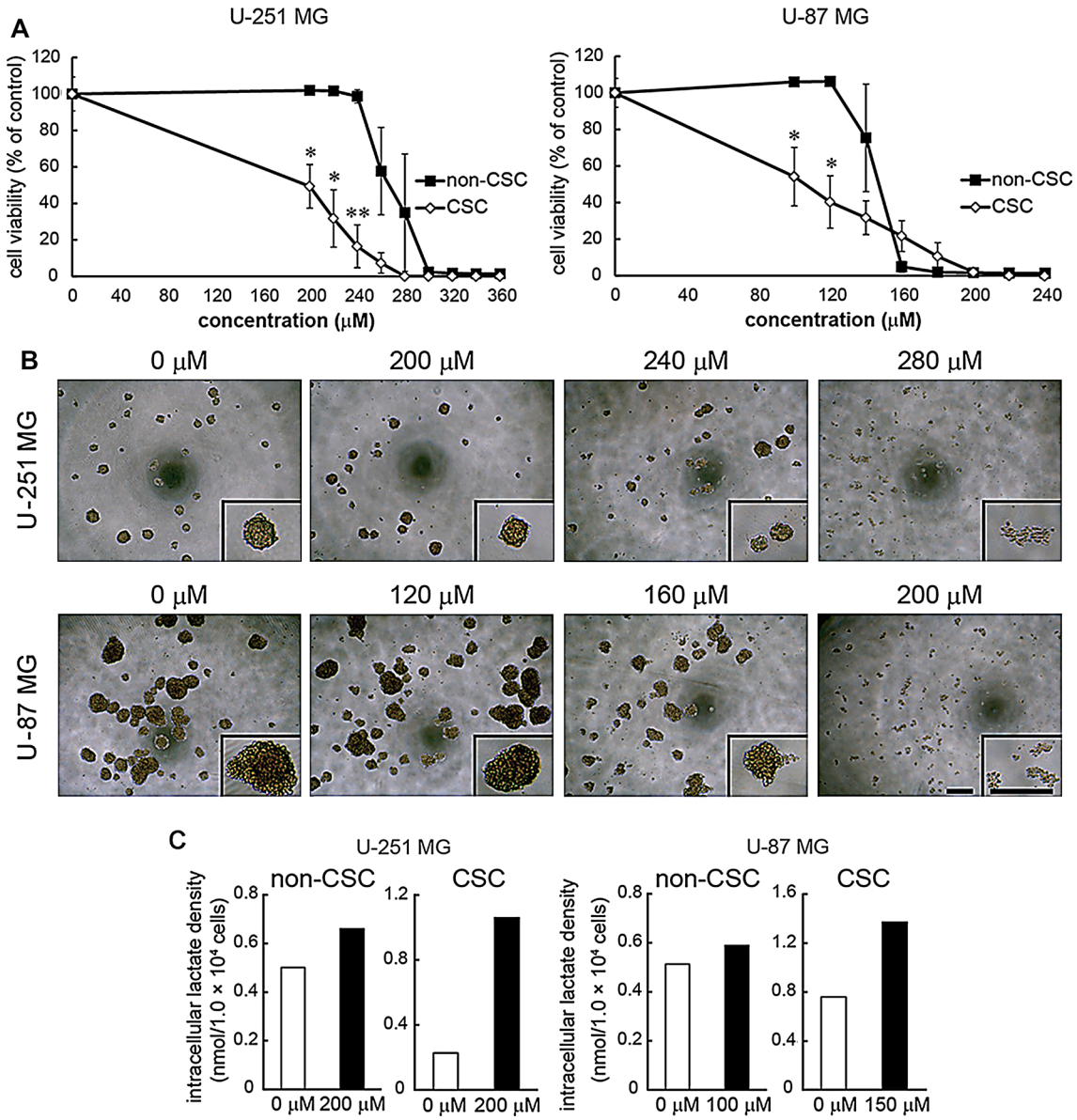

Fig. 3 Effect of pHMBS on non-CSCs and CSCs. **a** Cells were treated with pHMBS (U-251 MG: 200–360 μM, U-87 MG: 100–260 μM) or vehicle for 72 h ($n = 3$, mean ± SEM; $*p < 0.05$, $**p < 0.01$ vs. non-CSC of each concentration). **b** The number and size of spheres treated for 6 days with various concentrations of pHMBS. *Scale bars* 300 μm. **c** The intracellular lactate density (nmol/1.0 × 10^4 cells) of non-CSCs or CSCs treated with pHMBS for 72 h (non-CSCs) or 6 days (CSCs). These data are representative of two independent experiments. *CSC* cancer stem cell

CSCs and 200 μM in CSCs in U-251 MG cells, and approximately 150 μM in non-CSCs and 100 μM in CSCs in U-87 MG cells. Our results showed that pHMBS had a lower IC_{50} in CSCs than in non-CSCs. However, to show the full inhibitory effects, we used higher concentrations of pHMBS in CSCs than in non-CSCs of U-87 MG cells (Fig. 3a). The size of CSC spheres of U251-MG cells as well as U-87 MG cells became smaller by pHMBS treatment (Fig. 3b). We next examined the intracellular amounts of lactic acid using lactate assay. The pHMBS treatment accumulated much more lactic acid in CSCs normoxia than in non-CSCs normoxia. The intracellular lactate density in U251-MG CSCs under normoxic conditions increased to approximately 470 %, whereas that in U251-MG non-CSCs under normoxic conditions increased to approximately 130 %. The intracellular lactate density in U87-MG CSCs under normoxic conditions increased to approximately 170 %, whereas that in U87-MG non-CSCs under normoxic conditions increased to approximately 110 % (Fig. 3c).

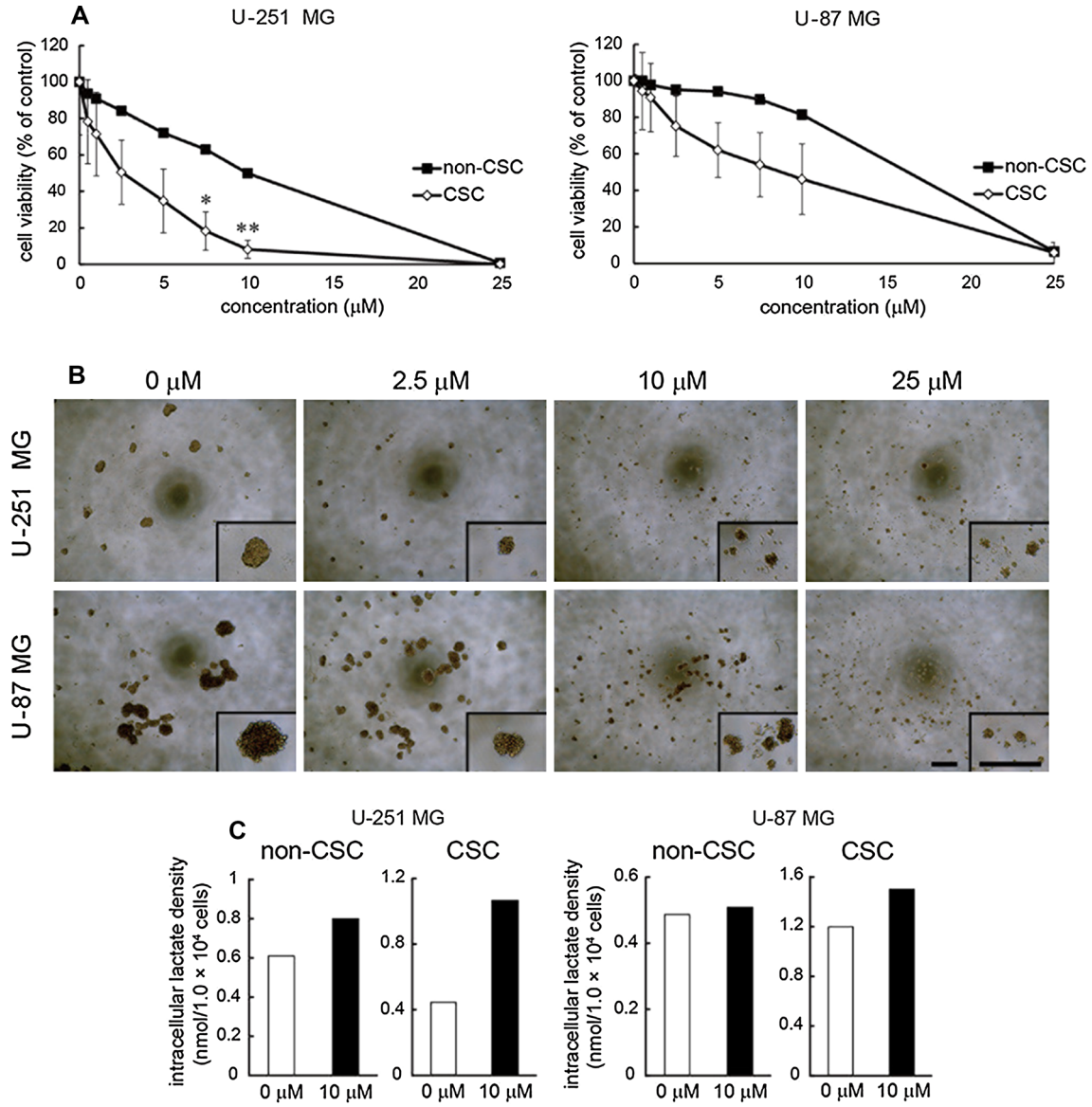

Fig. 4 Effects of AR-C117977 on non-CSCs and CSCs. **a** Cells were treated with AR-C117977 (0.5–25 μM) or 0.2 % DMSO (vehicle) for 72 h ($n = 3$, mean ± SEM; $*p < 0.05$, $**p < 0.01$ vs. non-CSC of each concentration). **b** The number and size of spheres treated for 6 days with various concentrations of AR-C117977. *Scale bars* 300 μm. **c** The intracellular lactate density (nmol/1.0 × 10^4 cells) of non-CSCs or CSCs treated with AR-C117977 for 72 h (non-CSC) or 6 days (CSC). These data are representative of two independent experiments. *CSC* cancer stem cell

AR-C117977 (MCT1 selective inhibitor) was more cytotoxic at lower concentrations in CSCs than in non-CSCs in each cell line and inhibited sphere formation

To analyze the effect of selective MCT1 inhibition, non-CSCs or CSCs of U-251 MG and U-87 MG cells were treated with AR-C117977. The IC_{50} was approximately 10 μM in non-CSCs and 2.5 μM in CSCs in U-251 MG cells, and approximately 15 μM in non-CSCs and 10 μM in CSCs in U-87 MG cells. These results indicated that AR-C117977 treatment reduced cell viability at lower concentrations in CSCs than in non-CSCs (Fig. 4a). The maximum diameter of spheres decreased in response to AR-C117977 in a dose-dependent manner (Fig. 4b). In the analysis of the intracellular lactic acid density, AR-C117977 also increased the intracellular lactic acid contents, and more lactic acid was accumulated in CSCs normoxia than in non-CSCs normoxia. The intracellular lactate density in U251-MG CSCs under normoxic conditions increased to approximately 240 %, whereas that in U251-MG non-CSCs under normoxic conditions increased

to approximately 130 %. The intracellular lactate density in U87-MG CSCs under normoxic conditions increased to approximately 120 %, whereas that in U87-MG non-CSCs under normoxic conditions increased to approximately 105 % (Fig. 4c). These observations suggest that MCT1 plays a more important role in the maintenance of homeostasis in GSCs.

Discussion

The present study indicates that the HA cells or CSCs from glioblastoma cells induced changes in the expression levels of various ion transport-related molecules. In particular, the conversion of cancer cells to CSCs induced the upregulation of *CA9*, *CA12*, and *MCT1*, whereas the conversion to HA cells induced *CA9* upregulation in U-251 MG and U-87 MG cells, as reported previously [24]. Immunofluorescence analysis showed the accumulation of pimonidazole in spheres, which suggested that intracellular conditions were hypoxic (Fig. 1d). The increased expression level of *CA9* in CSCs was induced by the hypoxic environment of spheres. In addition, the CSCs hypoxia could not induce the upregulation of *CA12* and *MCT1* by so much. However, *CA9* was further upregulated in CSCs hypoxia (Fig. S1). These results suggested that *MCT1*, which was upregulated only during the conversion of non-CSCs to CSCs, plays an important role in the maintenance of CSCs (Fig. S2). In this study, we used b-FGF and EGF to produce CSC spheres. This is a common technique used to examine the function of cancer stem cells [22, 23]. However, the detailed mechanism of how these cytokines act on MCT1 expression has not been clarified. Suzuki et al. showed that b-FGF and EGF promote the uptake of Glutamate by upregulating the glial glutamate transporter (GLAST) [25]. Therefore, we speculate that b-FGF and EGF signaling might also upregulate MCT1 expression. Consequently, glioblastoma stem cells (GSCs) have higher sensitivity to MCT1 inhibition as shown below. However, the accurate mechanisms have yet to be clarified. A previous study identified 14 MCT isoforms, including the three isoforms MCT1, MCT2, and MCT4, which are expressed in the brain [26]. MCT1 is expressed in astrocytes, endothelial cells of capillaries, and oligodendrocytes; MCT4 is primarily expressed in astrocytes, whereas MCT2 is expressed in neurons [26]. In addition, MCT1 and MCT4 control the release of lactic acid from astrocytes, and MCT2 controls the uptake of lactic acid into neurons [26].

We first examined the inhibiting effect of pHMBS, which inhibits MCT1 and MCT4 by binding to their cofactor CD147 (basigin) [27–30]. The observations that the size of CSC spheres of each cell lines became smaller by pHMBS treatment suggests that this inhibitor caused cell death because the cells are unable to maintain homeostasis [31, 32], which is in turn associated with the inhibition of the release of lactic acid. In CSCs normoxia, pHMBS decreased the sphere-forming ability and induced cell death earlier than non-CSCs normoxia. However, a higher concentration of pHMBS was needed to completely induce CSC death in U-87 MG cells than in non-CSCs. The concentration of pHMBS required to induce cell death in U-251 MG cells (approximately 200 μM) was higher than that required to induce cell death in U-87 MG cells (approximately 100 μM). We think that this is because the expression levels of MCT1 and MCT4 in U-87 MG cells were low compared with those in U-251 MG cells (Fig. S1). These data indicate that the dispersion effect depends on the type of glioblastoma.

We next examined the effect of selectively inhibiting MCT1 by AR-C117977, which was recently developed as an immunosuppressant and selectively binds to and inhibits MCT1 [33, 34]. In CSCs, AR-C117977 inhibited the sphere-forming ability, and cell death was induced earlier than in non-CSCs at all concentrations. These results showed an inverse correlation to the expression level of *MCT1*: higher *MCT1* expressing cells showed cell death at lower concentrations by AR-C117977. For the expression in the plasma membrane, MCTs require binding partners: CD147 (basigin) and gp70 (embigin). MCT1 associates with gp70 (embigin) in spite of the absence of CD147 [35]. pHMBS inhibits both MCT1 and MCT4 by binding to CD147 (basigin), and therefore pHMBS cannot inhibit MCT1 sufficiently. In contrast, AR-C117977 directly inhibits MCT1 [34]. Taken together, we speculate that a specific MCT1 inhibitor AR-C117977 is more effective in cells maintaining CSC homeostasis through MCT1. Furthermore, MCT1 inhibition induces the accumulation of protons in the cytoplasm, resulting in the acidification of GSCs. Because the accumulation of protons as well as Cl ions, which are counter ions of protons, is associated with cellular functions including migration and autophagy [36–38], the intracellular acidification might also induce cell death. We think that selective inhibition of MCT1 can decrease side effects in therapy because MCTs express the various organs not only brain and tumor [26]. pHMBS and AR-C117977 were used in animal studies in several reports, and no significant side effects were reported [27, 28, 30, 33]. However, when considering the clinical settings, pHMBS might be inappropriate because it contains mercury. Moreover, a phase I clinical trial of AZD3965, a MCT1 selective inhibitor, has started in patients with advanced cancer (NCT01791595). Therefore, we think that MCT1 selective inhibitors are safe in a clinical setting.

In conclusion, the selective inhibition of MCT1 demonstrated cytotoxicity at low concentrations in glioblastoma cells against inhibition of MCT and was

highly effective against glioblastoma-derived CSCs. These findings suggest that MCT1 selective inhibitors are useful as targeted therapeutic agents against GSCs.

Acknowledgments This work was supported by a Grant-in-Aid from the Ministry of Education, Culture, Sports, Science and Technology of Japan (23591404, 26461436 to EA) and a Grant-in-Aid from the Salt Science Research Foundation (1120 to EA).

Compliance with ethical standards

Conflict of interest T. Takada, K. Takata, and E. Ashihara disclose no financial conflicts of interest.

References

1. Singh SK, Hawkins C, Clarke ID et al (2004) Identification of human brain tumour initiating cells. Nature 432:396–401
2. Singh SK, Clarke ID, Terasaki M, Bonn VE, Hawkins C, Squire J (2003) Identification of a Cancer Stem Cell in Human Brain Tumors. Pathobiology 63:5821–5828
3. Bonnet D, Dick JE (1997) Human acute myeloid leukemia is organized as a hierarchy that originates from a primitive hematopoietic cell. Nat Med 3:730–737
4. Hemmati HD, Nakano I, Lazareff JA, Masterman-Smith M, Geschwind DH, Bronner-Fraser M, Kornblum HI (2003) Cancerous stem cells can arise from pediatric brain tumors. Proc Natl Acad Sci USA 100:15178–15183
5. Ohgaki H (2009) Epidemiology of brain tumors. Methods Mol Biol 472:323–342
6. Furnari FB, Fenton T, Bachoo RM et al (2007) Malignant astrocytic glioma: genetics, biology, and paths to treatment. Genes Dev 21:2683–2710
7. Sunayama J, Matsuda K-I, Sato A et al (2010) Crosstalk between the PI3 K/mTOR and MEK/ERK pathways involved in the maintenance of self-renewal and tumorigenicity of glioblastoma stem-like cells. Stem Cells 28:1930–1939
8. Sorensen MD, Fosmark S, Hellwege S, Beier D, Kristensen BW, Beier CP (2015) Chemoresistance and chemotherapy targeting stem-like cells in malignant glioma. Adv Exp Med Biol 853:111–138
9. Kalkan R (2015) Glioblastoma stem cells as a new therapeutic target for Glioblastoma. Clin Med Insights Oncol 9:95–103
10. Koppenol WH, Bounds PL, Dang CV (2011) Otto Warburg's contributions to current concepts of cancer metabolism. Nat Rev Cancer 11:325–337
11. Lindner D, Raghavan D (2009) Intra-tumoural extra-cellular pH: a useful parameter of response to chemotherapy in syngeneic tumour lines. Br J Cancer 100:1287–1291
12. Yang W, Zheng Y, Xia Y et al (2012) ERK1/2-dependent phosphorylation and nuclear translocation of PKM2 promotes the Warburg effect. Nat Cell Biol 14:1295–1304
13. Wojtkowiak JW, Verduzco D, Schramm KJ, Gillies RJ (2011) Drug resistance and cellular adaptation to tumor acidic pH microenvironment. Mol Pharm 8:2032–2038
14. Gallagher SM, Castorino JJ, Wang D, Philp NJ (2007) Monocarboxylate transporter 4 regulates maturation and trafficking of CD147 to the plasma membrane in the metastatic breast cancer cell line MDA-MB-231. Cancer Res 67:4182–4189
15. Guan B, Hoque A, Xu X (2014) Amiloride and guggulsterone suppression of esophageal cancer cell growth in vitro and in nude mouse xenografts. Front Biol (Beijing) 9:75–81
16. Cianchi F, Vinci M, Supuran C (2010) Selective inhibition of carbonic anhydrase IX decreases cell proliferation and induces ceramide-mediated apoptosis in human cancer cells. J Pharmacol Exp Ther 334:710–719
17. Sonveaux P, Végran F (2008) Targeting lactate-fueled respiration selectively kills hypoxic tumor cells in mice. J Clin Invest 118:3930–3942
18. Hosogi S, Miyazaki H, Nakajima KI, Ashihara E, Niisato N, Kusuzaki K, Marunaka Y (2012) An inhibitor of Na^+/H^+ exchanger (NHE), ethyl-isopropyl amiloride (EIPA), diminishes proliferation of MKN28 human gastric cancer cells by decreasing the cytosolic Cl^- concentration via DIDS-sensitive pathways. Cell Physiol Biochem 30:1241–1253
19. Supuran CT (2008) Carbonic anhydrases: novel therapeutic applications for inhibitors and activators. Nat Rev Drug Discov 7:168–181
20. Doyen J, Trastour C, Ettore F et al (2014) Expression of the hypoxia-inducible monocarboxylate transporter MCT4 is increased in triple negative breast cancer and correlates independently with clinical outcome. Biochem Biophys Res Commun 451:54–61
21. Koh MY, Powis G (2012) Passing the baton: the HIF switch. Trends Biochem Sci 37:364–372
22. Inoue A, Takahashi H, Harada H et al (2010) Cancer stem-like cells of glioblastoma characteristically express MMP-13 and display highly invasive activity. Int J Oncol 37:1121–1131
23. Yu S-C, Ping Y-F, Yi L et al (2008) Isolation and characterization of cancer stem cells from a human glioblastoma cell line U87. Cancer Lett 265:124–134
24. Chiche J, Ilc K, Laferrière J et al (2009) Hypoxia-inducible carbonic anhydrase IX and XII promote tumor cell growth by counteracting acidosis through the regulation of the intracellular pH. Cancer Res 69:358–368
25. Suzuki K, Ikegaya Y, Matsuura S, Kanai Y, Endou H, Matsuki N (2001) Transient upregulation of the glial glutamate transporter GLAST in response to fibroblast growth factor, insulin-like growth factor and epidermal growth factor in cultured astrocytes. J Cell Sci 114:3717–3725
26. Pierre K, Pellerin L (2005) Monocarboxylate transporters in the central nervous system: distribution, regulation and function. J Neurochem 94:1–14
27. Manning Fox JE, Meredith D, Halestrap AP (2000) Characterisation of human monocarboxylate transporter 4 substantiates its role in lactic acid efflux from skeletal muscle. J Physiol 529:285–293
28. Kirat D, Masuoka J, Hayashi H, Iwano H, Yokota H, Taniyama H, Kato S (2006) Monocarboxylate transporter 1 (MCT1) plays a direct role in short-chain fatty acids absorption in caprine rumen. J Physiol 576:635–647
29. Wilson MC, Meredith D, Fox JEM, Manoharan C, Davies AJ, Halestrap AP (2005) Basigin (CD147) Is the Target for Organomercurial Inhibition of Monocarboxylate Transporter Isoforms 1 and 4: THE ANCILLARY PROTEIN FOR THE INSENSITIVE MCT2 IS EMBIGIN (gp70). J Biol Chem 280:27213–27221
30. Iwata K, Kinoshita M, Yamada S, Imamura T, Uenoyama Y, Tsukamura H, Maeda KI (2011) Involvement of brain ketone bodies and the noradrenergic pathway in diabetic hyperphagia in rats. J Physiol Sci 61:103–113
31. Webb BA, Chimenti M, Jacobson MP, Barber DL (2011) Dysregulated pH: a perfect storm for cancer progression. Nat Rev Cancer 11:671–677
32. Baba M, Inoue M, Itoh K, Nishizawa Y (2008) Blocking CD147 induces cell death in cancer cells through impairment of glycolytic energy metabolism. Biochem Biophys Res Commun 374:111–116

33. Påhlman C, Qi Z, Murray CM, Ferguson D, Bundick RV, Donald DK, Ekberg H (2013) Immunosuppressive properties of a series of novel inhibitors of the monocarboxylate transporter MCT-1. Transpl Int 26:22–29
34. Bueno V, Binet I, Steger U, Bundick R, Ferguson D, Murray C, Donald D, Wood K (2007) The specific monocarboxylate transporter (MCT1) inhibitor, AR-C117977, a novel immunosuppressant, prolongs allograft survival in the mouse. Transplantation 84:1204–1207
35. Ovens MJ, Manoharan C, Wilson MC, Murray CM, Halestrap AP (2010) The inhibition of monocarboxylate transporter 2 (MCT2) by AR-C155858 is modulated by the associated ancillary protein. Biochem J 431:217–225
36. Miyazaki H, Marunaka Y (2015) The molecular mechanism of intracellular Cl^- function in gastric cancer invasion and metastasis by regulating expression of cell adhesion molecules. J Physiol Sci 65(Suppl-1):72
37. Miyazaki H, Marunaka Y (2014) Regulatory mechanisms of the G1 to S phase cell cycle progression via changes in the intracellular concentration of Cl^- in MKN28 human gastric cancer cells. J Physiol Sci 64(Suppl-1):267
38. Hosogi S, Marunaka Y, Niisato N, Kusuzaki K, Miyazaki H (2014) Cytosolic chloride ion is a key factor in lysosomal acidification and function of autophagy in human gastric cancer cell. J Physiol Sci 64(Suppl-1):215